Operating Characteristics for a Linear Detector of CW Signals in Narrow-Band Gaussian Noise

By G. H. ROBERTSON

(Manuscript received July 14, 1966)

This article presents a set of curves that can be used to evaluate in detail over a wide range of operating conditions the performance of systems using envelope detectors to search for CW signals in narrow-band Gaussian noise. The charts discussed relate the probability, P_D, of detecting such signals to (i) the signal-power/noise-power ratio, S/N, (ii) the proportion of false detections, P_{FA}, and (iii) the number, M, of independent samples of the envelope of the combined signal and noise that are averaged in making one attempt at detection. The curves and scales were calculated and drawn entirely by computer. The computation program was designed so that nearly linear curves could be produced, thereby increasing the accuracy and ease of interpolation.

I. INTRODUCTION

The curves* given in this article relate statistical properties of the output of an envelope detector to the signal-power/noise-power ratio, S/N, of a CW signal in narrow-band Gaussian noise at the input.

The signal will be represented here by a finite section of a sine wave which may be divided further into segments, for convenience in processing, so that most of the signal energy will be contained in a relatively narrow band, comparable in width to the reciprocal of the segment length. A filter will be used to select the part of the spectrum in which the signal may be found. The output of this filter will be applied to an envelope detector, and the amplitude of the output of the detector will be measured. Only if the magnitude measured at this

* This work was supported by the U. S. Navy, Bureau of Ships under contract no. N600(63133)64940.

point exceeds a chosen threshold value will a signal be presumed present.

For other detection tests two or more samples of the output of the detector, taken far enough apart in time that the noise values are independent, will be averaged. Only if the value of such an average exceeds a chosen threshold will a signal be presumed present. The curves given here for the averages of multiple samples depend on the assumption that a detected signal remains steady while the samples are taken, and that the noise background is weakly stationary.

This form of detection criterion has been discussed by several authors,[1, 2, 3, 4] who give major emphasis to the use of a square-law detector because it is easier to analyze. A linear detector, however, is much more practical and is extensively used, so results that specifically apply to it are desirable.

The curves available in the literature are difficult to use for checking system performance at more than a few scattered points. Those given here, on the other hand, are believed to be suitable for defining system performance in detail over a considerable range of threshold values and, furthermore, are easy to use.

II. DISCUSSION OF THE MATHEMATICAL MODEL

We assume that the spectrum of noise in the vicinity of the signal is smooth enough so that the output of the filter can be considered a narrowband Gaussian process with the possible addition of a sinusoidal signal. S. O. Rice[5, 6] derived an expression for the probability density of the envelope of such a waveform. Rice's expression, paraphrased, is

$$P(\rho)\, d\rho = 2h^2\rho \exp\left[-h^2(r^2 + \rho^2)\right] I_0(2h^2 r\rho)\, d\rho \tag{1}$$

which gives the probability that the envelope lies within an interval, $d\rho$, of ρ. $P(\rho)$ is thus the probability density. $I_0(z)$ is the modified Bessel function of zero order defined by

$$I_0(z) = \sum_0^\infty \frac{(\frac{1}{2}z)^{2n}}{(n!)^2}. \tag{2}$$

Note that in (1) the term h^2r^2, which represents the signal/noise power ratio, and $1/\sqrt{2}h$, which represents the rms noise level, can be identified. In this article S/N always means the ratio of the signal power to the noise power accompanying it in the specified narrow band.

When there is no signal (1) becomes

$$P(\rho)\,d\rho = 2h^2\rho\exp(-h^2\rho^2)\,d\rho \tag{3}$$

which represents a Rayleigh distribution having

$$2\sigma^2 = 1/h^2 \tag{4}$$

for the second moment about zero.

The distribution of the envelope of the filter output is thus given by (1) when a signal is present, and by (3) when there is no signal. From these expressions distribution curves can be drawn for cases where only noise is present, and where a known signal occurs with the noise. To generate the performance charts given here, one has to be able to calculate the area lying above some threshold for distribution curves corresponding to no signal, and for those corresponding to all the values of S/N of interest.

Only in the case of noise alone, for single-sample detection, is it possible to get an explicit formula for the area under portions of such a curve. Moments of the distribution given in (1) can be calculated with the help of Ref. 7. We give here the nth moment about zero:

$$\begin{aligned} \nu_n &= \int_0^\infty P(\rho)\rho^n\,d\rho \\ &= 2\exp(-h^2r^2)\int_0^\infty h^2\rho^{n+1}\exp(-h^2\rho^2)I_0(2h^2r\rho)\,d\rho \\ &= (\sqrt{2}\sigma)^n\Gamma\left(\frac{n+2}{2}\right){}_1F_1\left(-\frac{n}{2}\,;1;-h^2r^2\right). \end{aligned} \tag{5}$$

In this h^2r^2 is the signal/noise power and

$$2\sigma^2 = 1/h^2$$

as stated earlier.

$\Gamma(z)$ is the Gamma function and ${}_1F_1\,(a;b;z)$ is the Confluent Hypergeometric function defined by

$${}_1F_1(a;b;z) = 1 + \frac{a}{b}\cdot\frac{z}{1} + \frac{a(a+1)}{b(b+1)}\cdot\frac{z^2}{2\cdot1} + \frac{a(a+1)(a+2)}{b(b+1)(b+2)}\cdot\frac{z^3}{3\cdot2\cdot1} + \cdots . \tag{6}$$

When the signal/noise power becomes zero we have

$$\nu_{0_n} = (\sqrt{2}\sigma)^n \Gamma\left(\frac{n+2}{2}\right). \tag{7}$$

This gives the nth moment about zero for the distribution due to noise alone. We therefore have

$$\nu_n = \nu_{0_n} {}_1F_1\left(-\frac{n}{2}\,;\,1\,;\,-h^2r^2\right) \tag{8}$$

which gives the nth zero moment of the distribution when $S/N = h^2r^2$. We can thus derive a type-A Gram-Charlier[8] (G-C) series approximation to the distribution curve for any S/N, and, since the series can be integrated, the area under any desired part of the curve can be found. Knowing the moments of the primary distribution, we can calculate the moments of a secondary distribution formed by averaging M samples of the primary distribution. We thus form a G-C series which can be integrated to get the area under any desired part of the secondary distribution curve.

Charts are included that cover cases in which, when only noise is present, the probability is as low as 10^{-6} that the threshold will be exceeded, even with the use of single samples in detection attempts.

Producing a G-C series that would give results within 1 percent of the true value when the threshold is great enough to give such a low probability required evaluating many more moments than is usual in G-C series. In fact, 31 moments were calculated, which resulted in a series that oscillates about the true value of the distribution as the threshold is varied. A method that sometimes reduces these oscillations is to use special groupings of the terms, forming a so-called Edgeworth series.[8] It occurred to the author, however, that a better fit might be obtained by averaging the approximations given by several G-C series carried out to different numbers of terms since their oscillations as the threshold varies are not in phase. This involves very little more work than deriving the series that has the most terms, since it merely requires that the terms be weighted to represent the number of times they occur in forming the average. Fig. 1 shows the results obtained by forming G-C series that use up to 31 moments and averaging over the highest 23 and 13 terms, respectively. Both show less oscillation over restricted—though appreciable—ranges of threshold than does the Edgeworth series that uses up to 30 moments. The curve showing

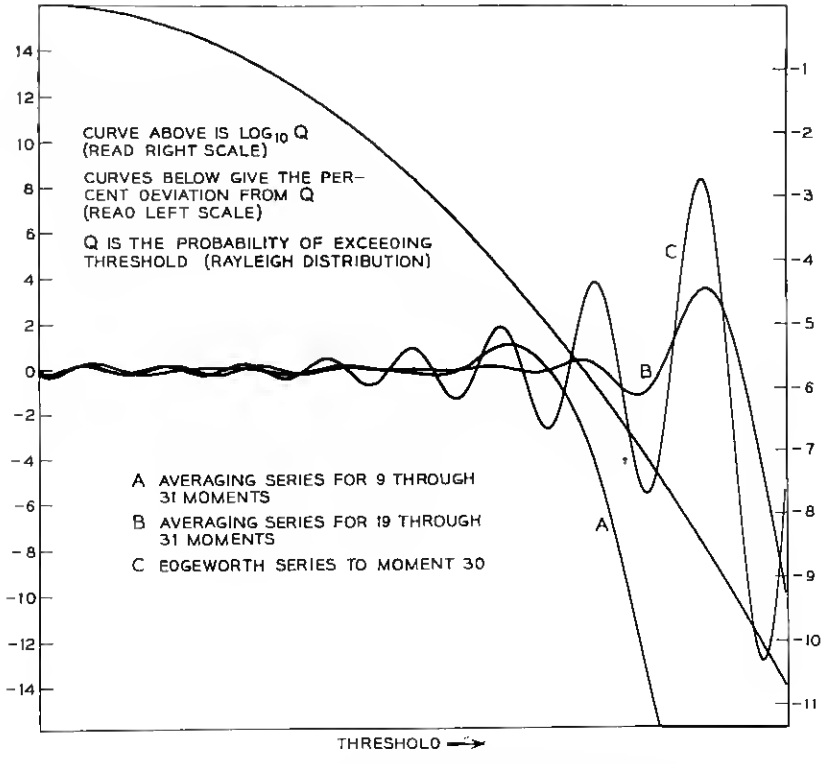

Fig. 1 — Comparison of methods for evaluating G-C series.

the logarithm of Q, the function approximated by the series, allows the useful range to be assessed. It makes possible the calibration of the horizontal scale, which is the same for all four curves, in terms of the probability that the threshold will be exceeded. The logarithm to the base ten of this probability is given by the right scale of Fig. 1.

III. DESCRIPTION OF THE CHARTS

We will now describe briefly how the charts (Figs. 2 through 15) were produced and point out their main features. Some of these are believed novel and show the advantage of being able to use a digital computer to generate and draw charts of this type.

For each value of S/N at which a curve was desired, the detection threshold, T, was expressed in two ways: (*i*) measured with respect

to the mean of the distribution for noise only, and standardized by dividing by the square root of the variance, and (*ii*) measured with respect to the mean of the distribution appropriate to the S/N, and standardized with respect to this distribution.

The form in (*i*) is appropriate for calculating the probability of false alarm (i.e., the probability that noise alone will cause the threshold to be exceeded), and the form in (*ii*) is appropriate for calculating the probability of detection (the probability that a signal at the chosen

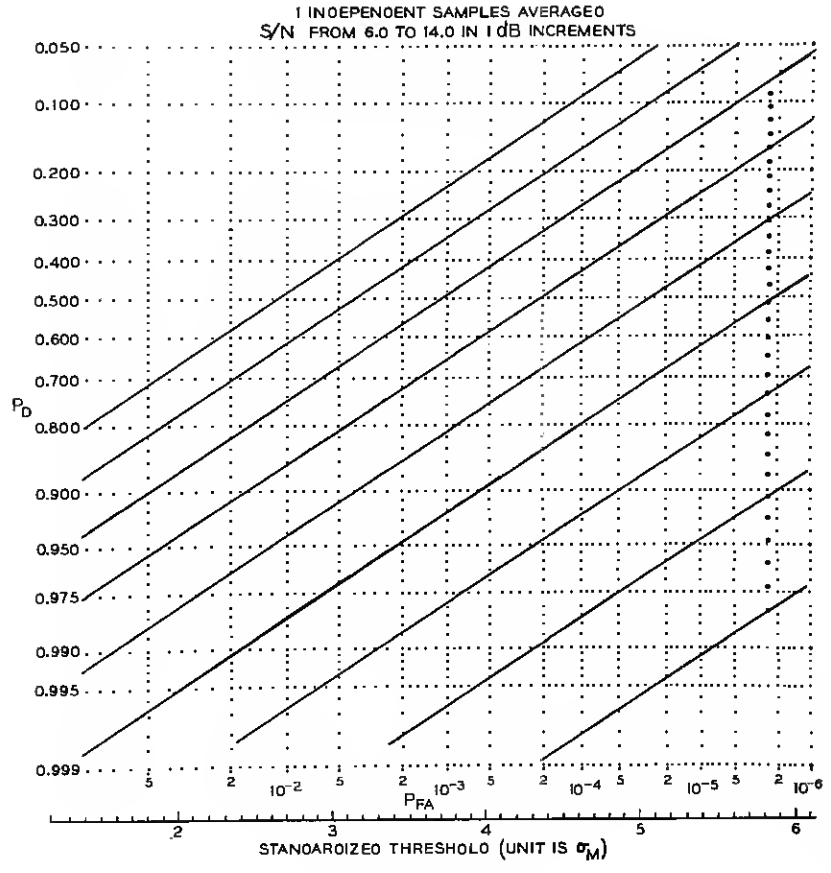

Fig. 2 — ROC curves.

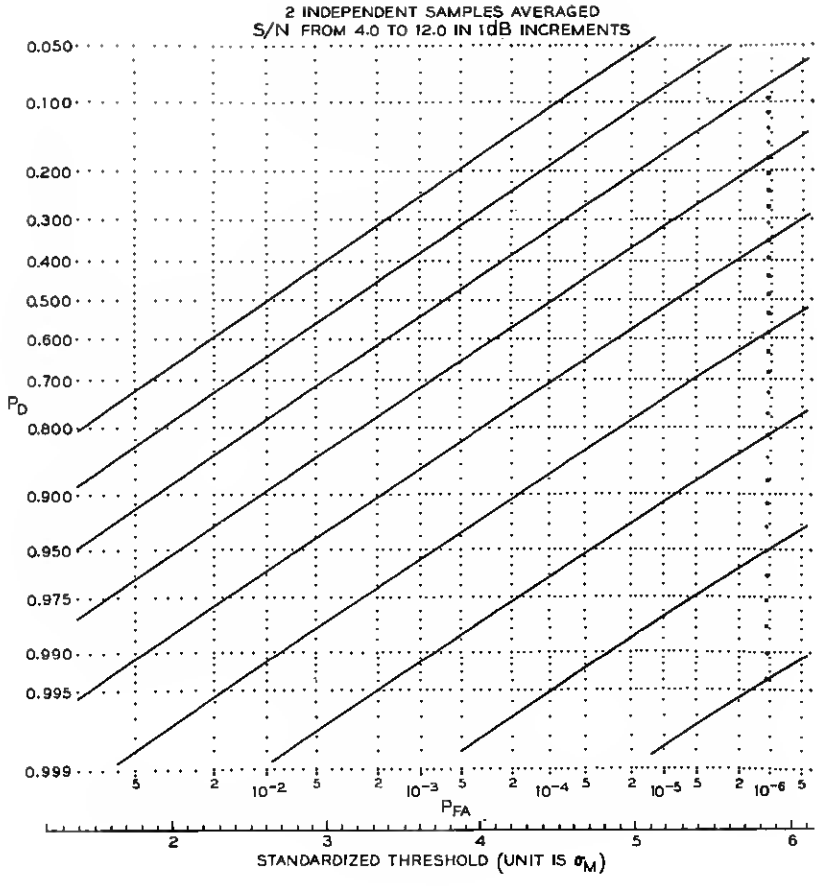

Fig. 3 — ROC curves.

S/N will cause the threshold to be exceeded). The relationship between these two forms is linear, so that if the threshold were varied a straight line would give the relationship between a scale for measuring the variation based on (*i*) and another based on (*ii*). If these scales were calibrated in terms of probability of false alarm, P_{FA}, and probability of detection, P_D, useful charts could be obtained that use these probability parameters as horizontal and vertical axes, respectively.

But, for any P_{FA} scale, the corresponding P_D scale depends on S/N. Fortunately, the P_D scale does not change rapidly with S/N for the range we are interested in, and, to allow several S/N values to be included on each chart, a constant normal probability scale was chosen for P_D. The penalty incurred by doing this is the slight curvature of some of the S/N lines plotted in Figs. 2 through 15.

It can be seen that the horizontal scale, P_{FA}, changes as the number of samples averaged changes. This is because the probability dis-

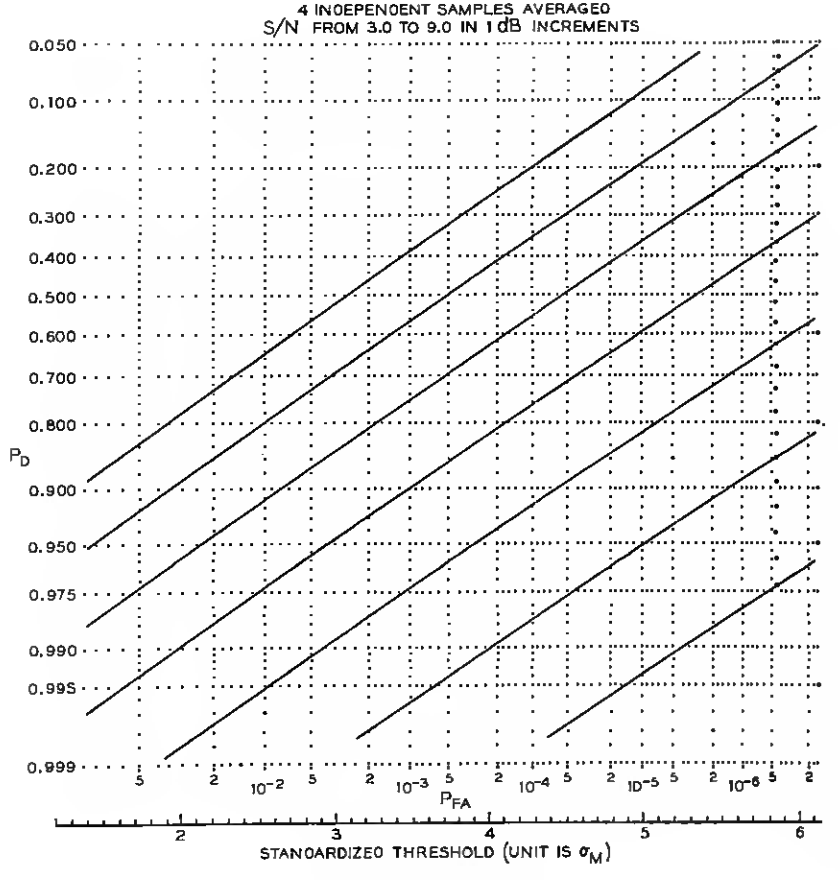

Fig. 4 — ROC curves.

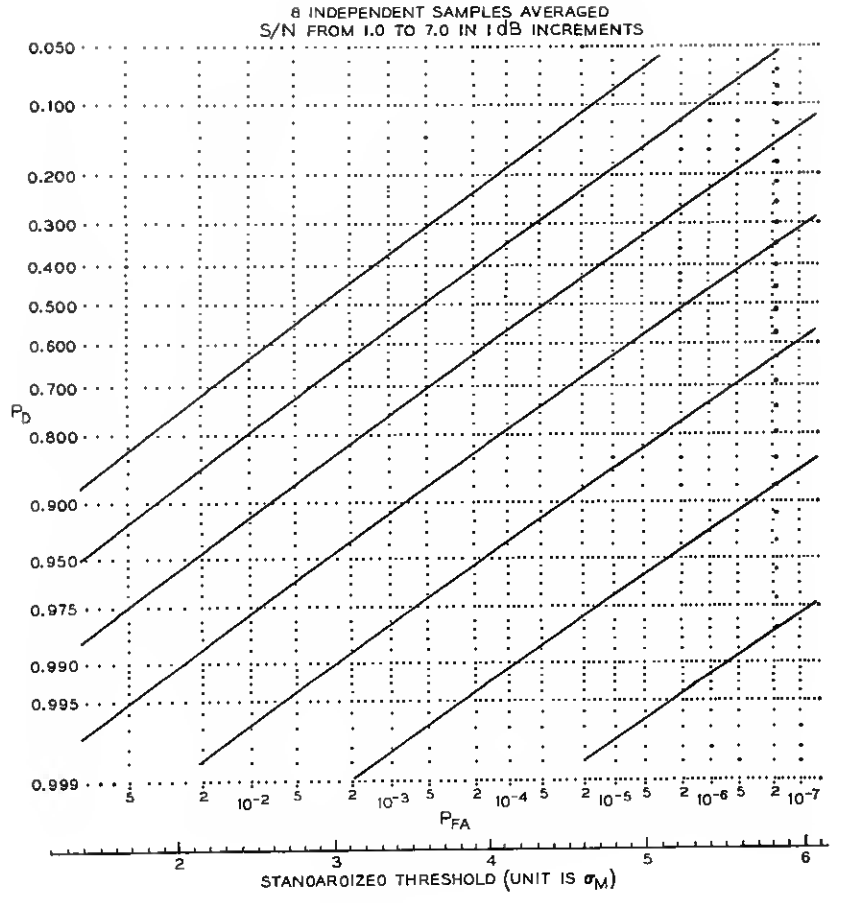

Fig. 5 — ROC curves.

tribution for the average of a number of samples depends on the number averaged as well as on the basic distribution. Since an explicit formula for the cumulative probability is known in the case of the basic (Rayleigh) distribution, the Rayleigh distribution was used to get the P_{FA} scale for the chart based on single-sample decisions. All the other scales were calculated from G-C series approximations to the appropriate distributions.

To make interpolation easier, a column of heavy dots was put near the right edge of each chart. These dots mark 0.2 dB increments in S/N between the lines. Since any two adjacent S/N lines are very nearly straight and parallel it is easy to interpolate to within 0.1 dB between the lines using a parallel ruler guided by the heavy dots.

The horizontal and vertical grids were plotted as rows and columns of dots in order to carry the accuracy of the scales into all parts of the chart without also producing a confusing mesh of lines.

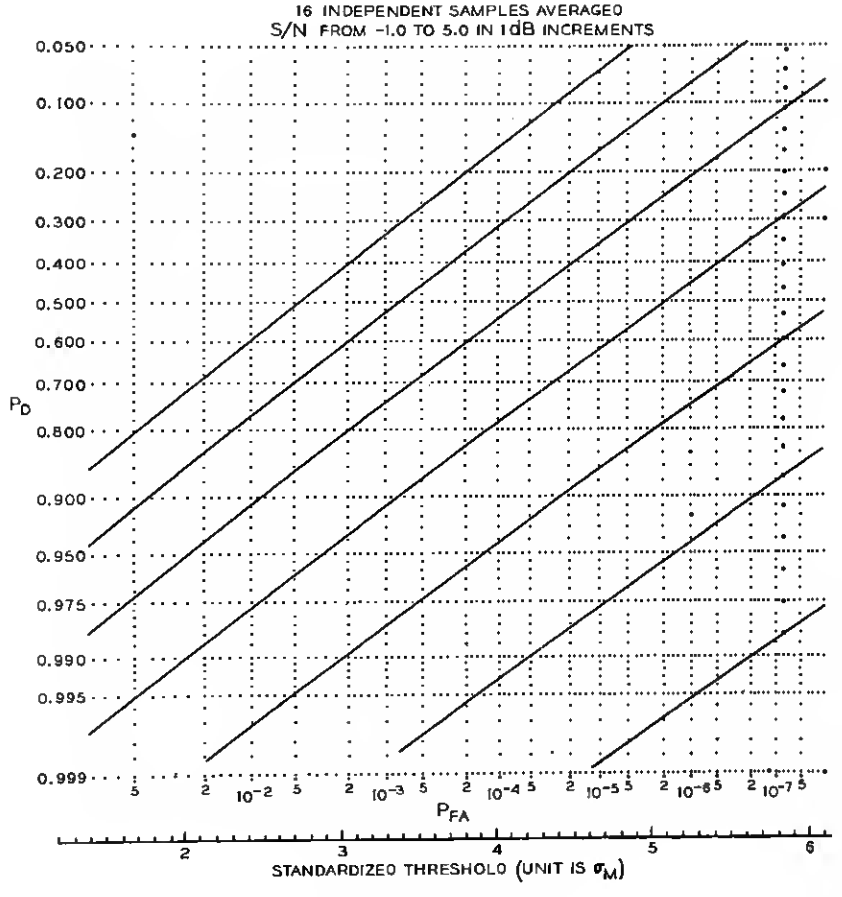

Fig. 6 — ROC curves.

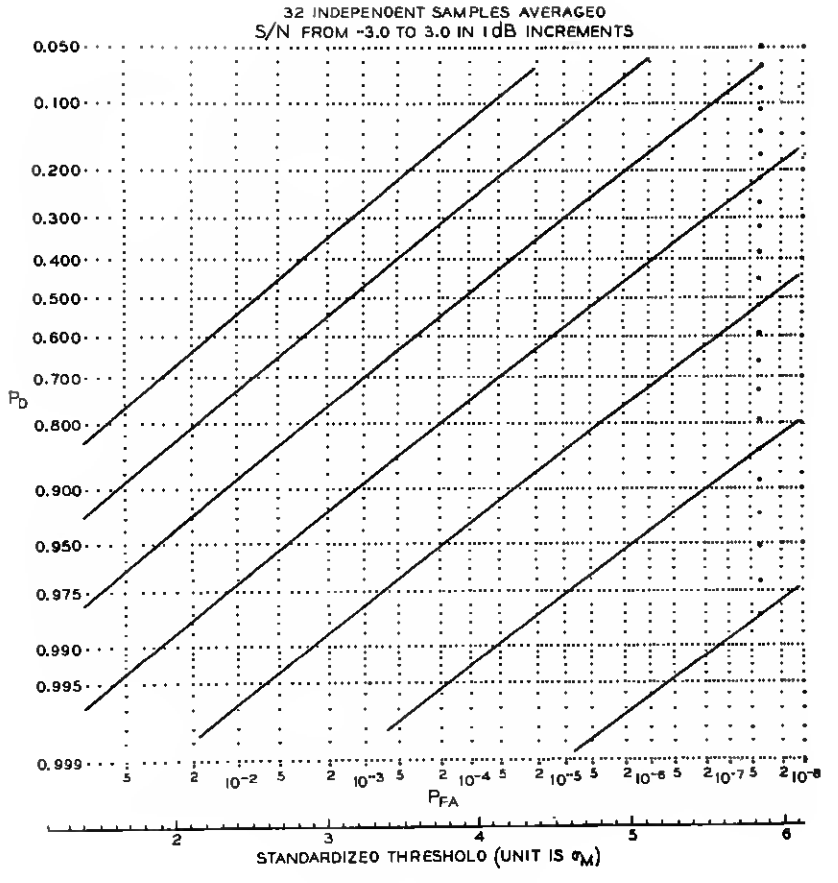

Fig. 7 — ROC curves.

Each decade of the horizontal, P_{FA} , scale, reading from left to right, is given by

$$10.0(1.0)4.0(0.5)2.0(0.2)1.0,$$

where the increments are in parentheses.

The vertical, P_D , scale, reading from top to bottom, is

$$0.05\,(0.01)\,0.10\,(0.02)\,0.90\,(0.01)\,0.950\,(0.005)\,0.980$$

$$0.980\,(0.0025)\,0.990\,(0.001)\,0.998\,(0.0005)\,0.999,$$

the increments again being in parentheses.

On Fig. 16 are curves for two pairs of P_D, P_{FA} values that show how the S/N for each pair varies with the logarithm to the base 2 of the

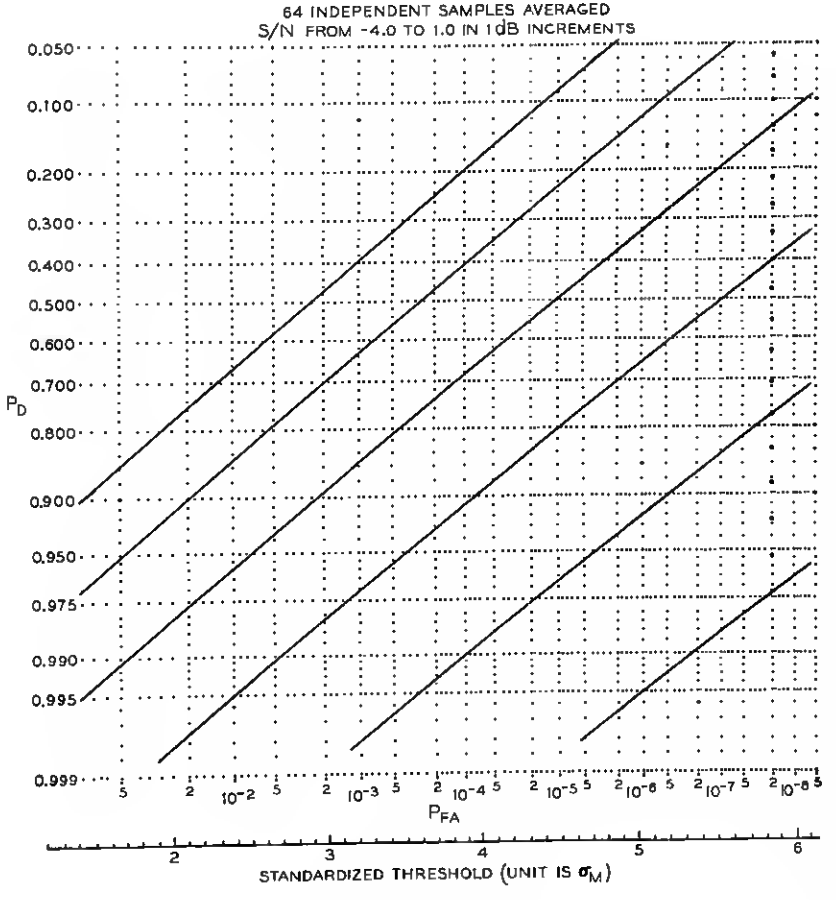

Fig. 8 — ROC curves.

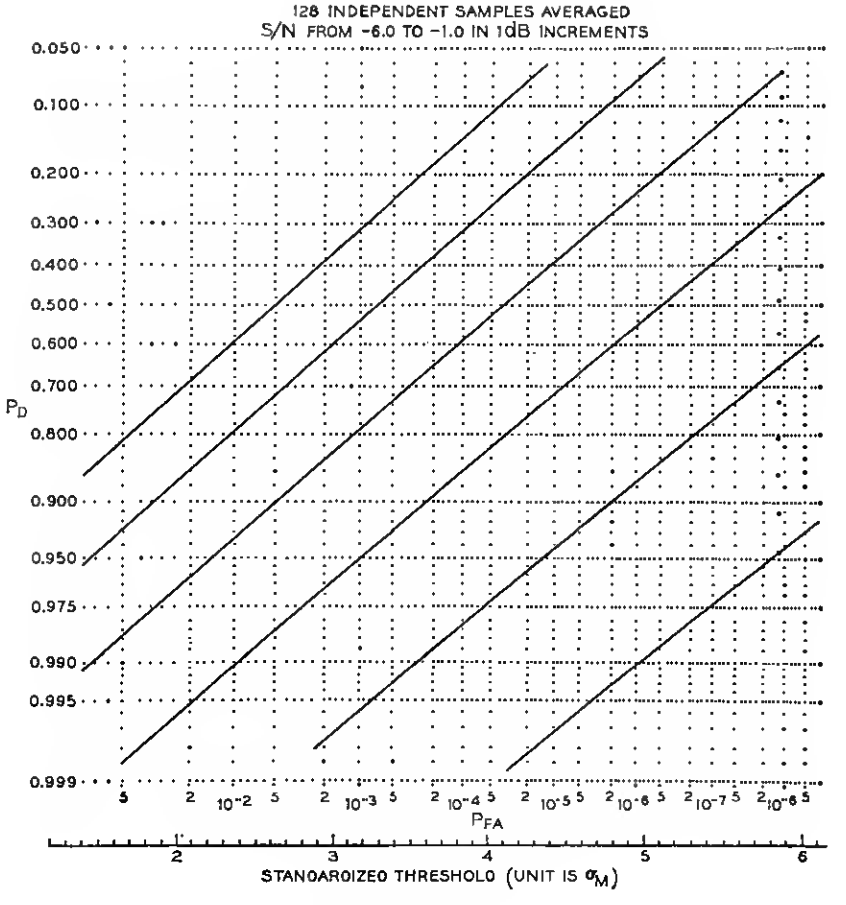

Fig. 9 — ROC curves.

number of samples averaged. Over any restricted range in which the number of samples is doubled, either curve could be approximated quite satisfactorily by a straight line.

The slopes of these two curves are almost the same at the same S/N, although the P_D, P_{FA} values are quite different. This means that, within any small range of P_D, P_{FA} values, curves like those shown in Fig. 16 can be assumed parallel with little sacrifice in accuracy. Con-

sequently, the change in S/N corresponding to a small change in $\log_2 M$ indicated by such a curve will hold quite accurately for a small range of P_D, P_{FA} values around the pair for which the curve is actually drawn.

The S/N corresponding to any pair of P_D, P_{FA} values can therefore be calculated for a different number of samples averaged by assuming a linear relationship between S/N and the logarithm to the base 2 of the number of samples.

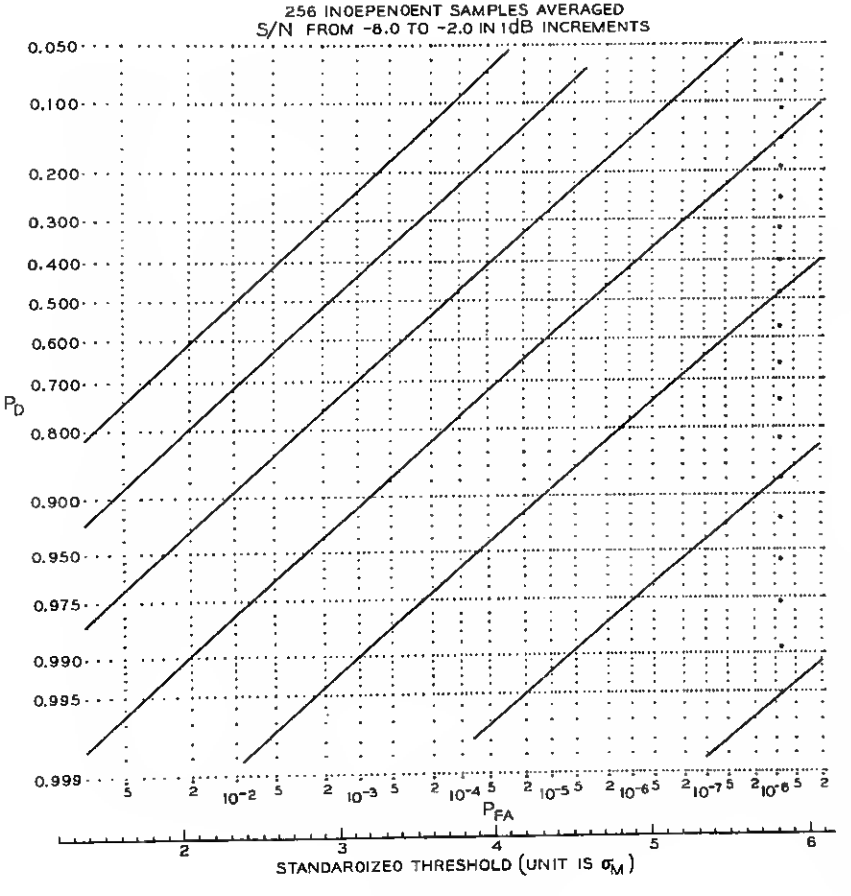

Fig. 10 — ROC curves.

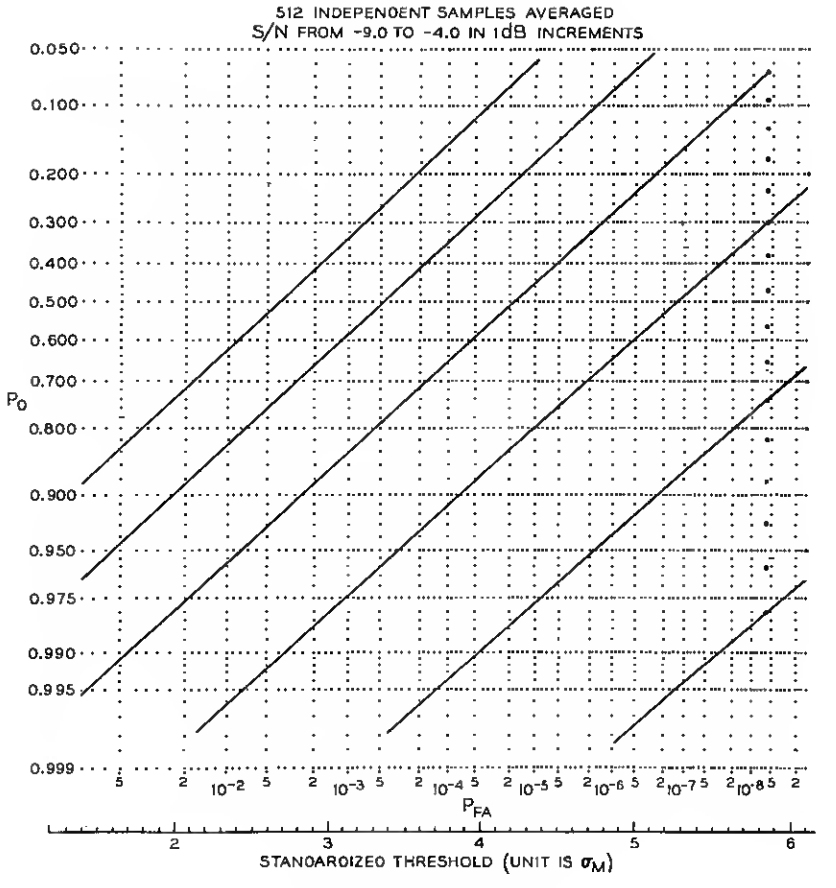

Fig. 11 — ROC curves.

IV. CONCLUSION

4.1 *Efficiency of Post-Detector Integration*

When more than one sample can be averaged to improve detection sensitivity the process is usually called post-detector integration. The curves of Fig. 16 show how efficient this process is at different values of S/N and P_D, P_{FA} operating points. The gradients of these curves show the rate at which detectability is improved, measured in dB/

double-the-number-of-samples, ds, for two operating points. This ratio is convenient to use in interpolating between adjacent charts, since the number of samples doubles from one chart to the next.

It can be seen that the gradients are almost the same where the S/N is the same. The rate of improvement is better than 2 dB/ds for S/N above 10 dB, presumably reaching a maximum of 3 dB/ds for high S/N. The rate apparently becomes constant at 1.5 dB/ds for S/N values less than −10 dB.

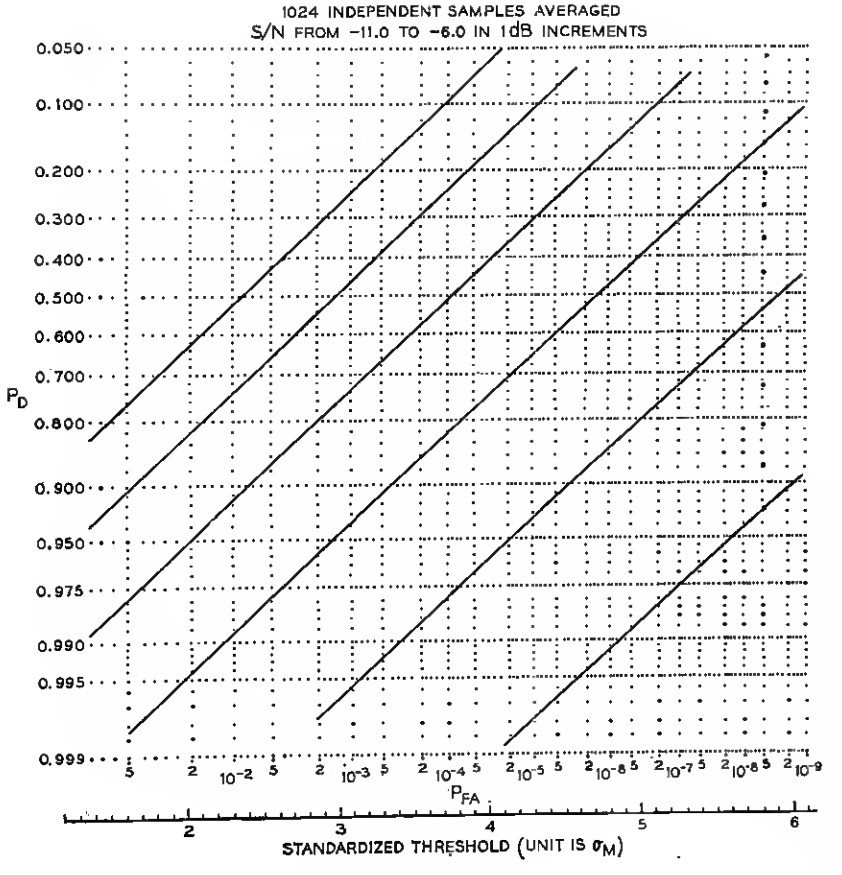

Fig. 12 — ROC curves.

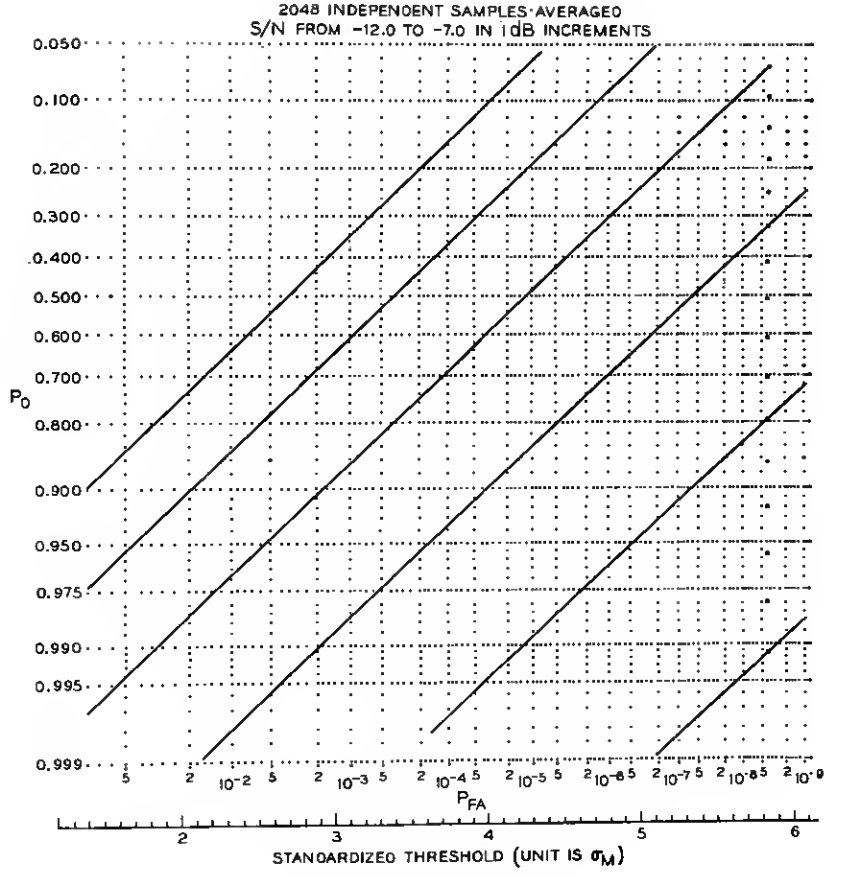

Fig. 13 — ROC curves.

4.2 *Extending the Scope of the Charts*

The detector input is restricted to a relatively narrow band of frequencies to ensure that the envelope can be measured accurately after detection. By bandshifting high enough, this result can be obtained even for bands of quite appreciable width. The charts can therefore be used in situations where the significant signals may be quite short bursts of nearly sinusoidal waveform.

The same standardized threshold scale applies to all the charts. It is given in units of

$$\sigma_M = \sigma/\sqrt{M}, \tag{9}$$

where σ is the rms noise into the detector and M independent samples are averaged.

Although the curves given here refer strictly to envelope detectors they can be applied when square-law-detectors are used if a small

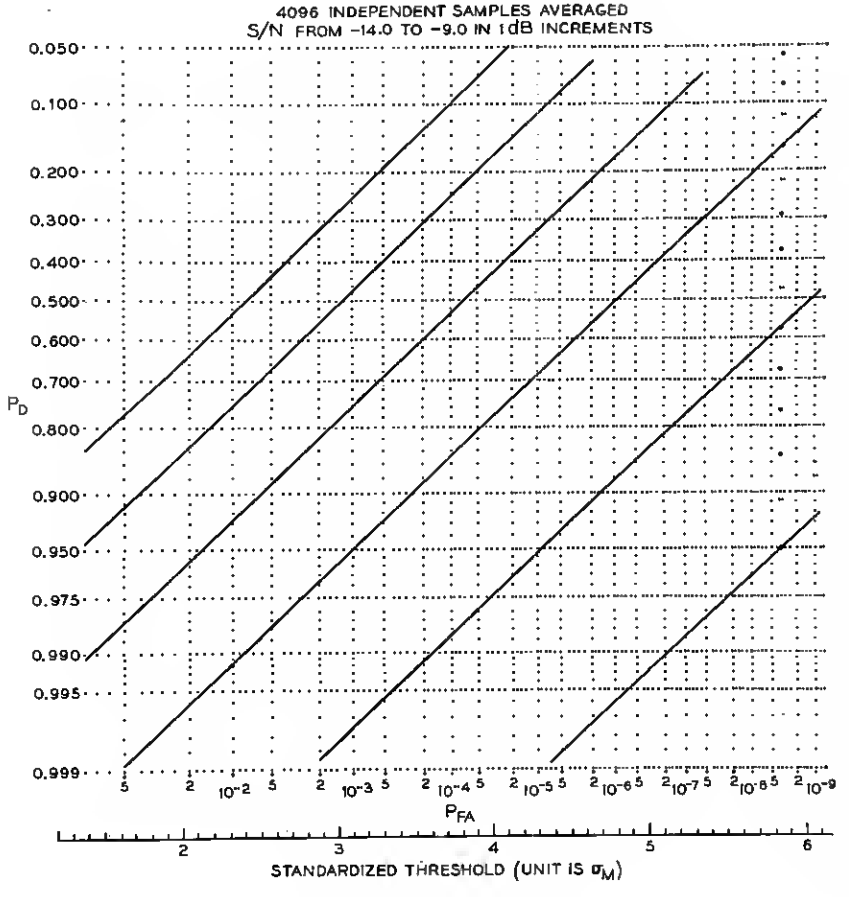

Fig. 14 — ROC curves.

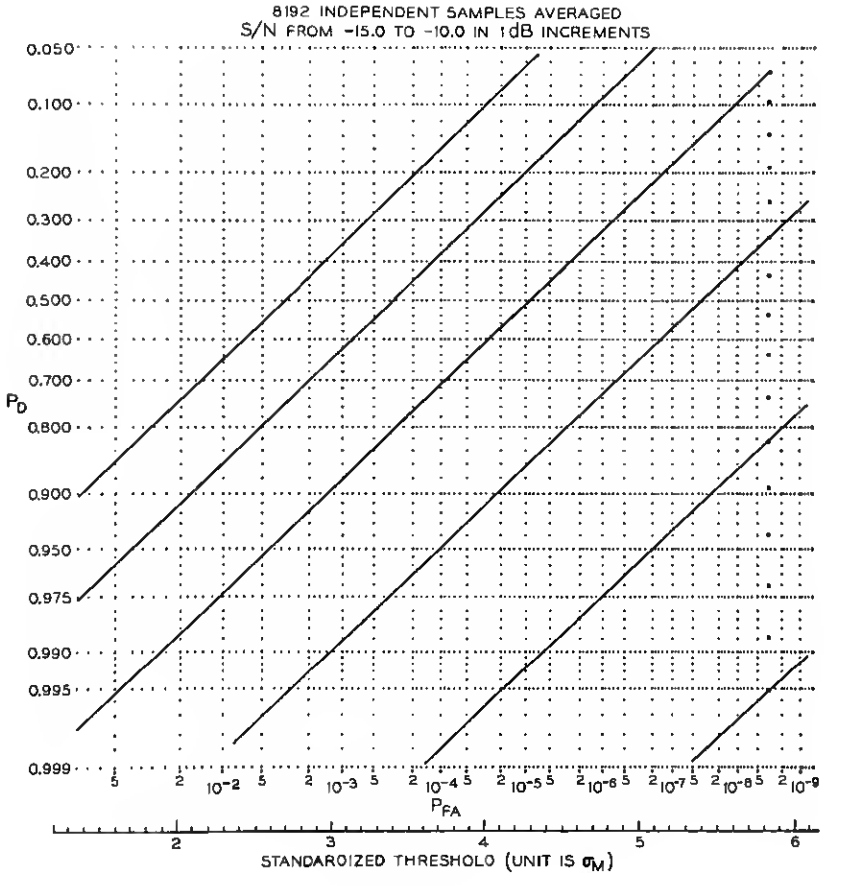

Fig. 15 — ROC curves.

error (always less than 0.2 dB) in S/N is taken into account, and the standardized threshold scale is changed. A calibration curve for this error is given in Ref. 1. Reasonable agreement with this curve was found by generating ROC curves for a square-law detector after suitably modifying the computer program. It was possible thus to get ROC curves for 1 sample and for averaging 128 or more independent samples.

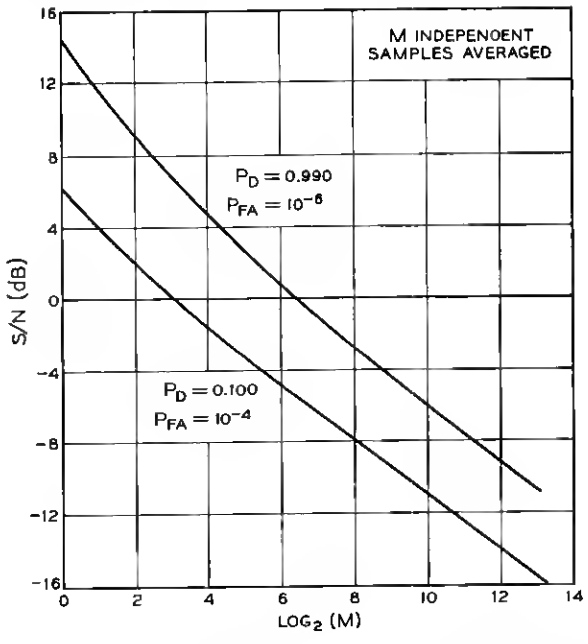

Fig. 16 — Sensitivity related to number of samples averaged.

REFERENCES

1. Marcum, J. I., A Statistical Theory of Target Detection by Pulsed Radar: Mathematical Appendix, *Research Memorandum RM-753*, The Rand Corporation, July 1, 1946.
2. Schwartz, M., A Statistical Approach to the Automatic Search Problem, Harvard University Dissertation, May 1, 1951.
3. Peterson, W. W., Birdsall, T. G., and Fox, W. C., The Theory of Signal Detectability, 1954 Symposium on Information Theory, IRE Trans. PGIT, *IT-4*, September, 1954, pp. 171–212.
4. Kaplan, E. L., Signal-Detection Studies with Applications, B.S.T.J., *34*, March, 1955, pp. 403–437.
5. Rice, S. O., Mathematical Analysis of Random Noise, B.S.T.J., *24*, January, 1945, pp. 46–156, Section 3.10.
6. Rice, S. O., Properties of a Sine Wave Plus Random Noise, B.S.T.J., *27*, January, 1948, pp. 109–157, Section 3.
7. Ryshik, I. M. and Gradstein, I. S., *Tables of Series Products and Integrals*, 2nd Ed., Plenum Press, 1963, Formula 4.434.
8. Fry, T. C., *Probability and Its Engineering Uses*, Van Nostrand, 2nd Ed., 1965, Sections 124 through 127.